Islands of Runaway Electrons in the TEXTOR Tokamak and Relation to Transport in a Stochastic Field

R. Jaspers,[1] N. J. Lopes Cardozo,[1] K. H. Finken,[2] B. C. Schokker,[1] G. Mank,[2] G. Fuchs,[2] and F. C. Schüller[1]
[1]*FOM-Instituut voor Plasmafysica "Rijnhuizen," P.O. Box 1207, 3402 BE Nieuwegein, The Netherlands*
[2]*Institut für Plasmaphysik, Forschungszentrum Jülich, D-52425 Jülich, Germany*
(Received 1 December 1993)

A population of 30 MeV runaway electrons in the TEXTOR tokamak is diagnosed by their synchrotron emission. During pellet injection a large fraction of the population is lost within 600 μs. This rapid loss is attributed to stochastization of the magnetic field. The remaining runaways form a narrow, helical beam at the $q = 1$ drift surface. The radial and poloidal diffusion of this beam is extremely slow, $D < 0.02$ m^2/s. The fact that the beam survives the period of stochastic field shows that in the chaotic sea big magnetic islands must remain intact.

PACS numbers: 52.55.Fa, 52.35.Ra

The fact that the mean free path of an electron in a plasma is a strongly increasing function of its velocity gives rise to the phenomenon of electron runaway. In an electric field, electrons which exceed a critical velocity, for which the collisional drag balances the acceleration by the field, are accelerated freely and can reach very high energies. In low density tokamak discharges a considerable amount of runaway electrons with energies up to tens of MeV can thus be created. As these energetic electrons are effectively collisionless, they follow the magnetic field lines and can therefore been used to probe the magnetic turbulence in the core of the plasma [1].

In the TEXTOR tokamak a helical beam of runaway electrons is observed after injection of a deuterium pellet. This paper deals with the implications for transport and magnetic turbulence that can be deduced from the synchrotron radiation in these experiments. Before pellet injection, the runaway electrons have been confined for more than 1 s, which is evident from the high energies of several tens of MeV these electrons have acquired and also from their exponentially growing population, which results from secondary generation [2]. During the pellet injection a rapid loss of most of these runaways is observed, however, a part of them does survive the event and forms a stable and narrow beam.

In the TEXTOR tokamak (major radius $R_0 = 1.75$ m, minor radius $a = 0.46$ m, toroidal magnetic field $B_T =$ 2.25 T, plasma current $I_P = 350$ kA; circular cross section) runaway electrons with energies up to 30 MeV have been observed directly with an infrared (IR) camera, which measures the synchrotron radiation in the wavelength range 3–14 μm [3]. The camera is positioned to view the plasma in toroidal direction towards electron approach. This camera uses a single HgCdTe detector and a horizontally and a vertically scanning mirror. The scanning follows the NTSC-TV standard, i.e., a full 2D picture is obtained every 1/60 s, or as an alternative by scanning only one mirror, a 1D line is obtained every 64 μs [4]. Detectable numbers of runaways are routinely produced in low density discharges with electron density $n_e <$ 10^{19} m^{-3}. The runaway energy E can be deduced from the spectrum, the pitch angle θ (ratio of the velocities perpendicular and parallel to the magnetic field) from the shape of the 2D image, and the total number of runaways N from the absolute intensity [3]. Measurements of the extension of the runaway population were hampered by the limited field of view which covers a fraction of the plasma cross section mainly on the high field side, where synchrotron radiation was observed up to $r = -20$ cm.

Observations.—During the steady state phase of a discharge, the IR picture changes only slowly, corresponding to the growth of the runaway population. It has been shown [2] that the runaway electrons are born throughout the discharge duration, and that the rate of runaway production is in agreement with the theory of secondary generation, being the process in which already existing high energy runaway electrons push thermal electrons beyond the critical velocity by collisions [5]. The runaway energy saturates at the level where the radiation loss matches the acceleration in the electric field. Typical results in the steady state before pellet injection are [2, 3] $E = 25$ MeV, $\theta = 0.12$, $N = (1-30) \times 10^{14}$. The large spread in the number of runaways arises from the unknown energy distribution of these particles.

After the synchrotron radiation is well established, i.e., at $t = 2.5$ s, a deuterium pellet is injected horizontally into the midplane with $v \approx 1200$ m/s whereby one pellet contains $\approx (1-2) \times 10^{20}$ atoms. As a result, the density increases by a factor of 2–3. The injection of the pellet is followed by oscillations with frequencies in the range of 0.2–2 kHz, observed on magnetics, density, ECE, and hard x-ray signals, as shown in Fig. 1. The most dominant magnetic mode normally seen in TEXTOR is the $n = 1$, $m = 1$ mode if the pellet has penetrated far enough to reach the $q = 1$ surface [6], but for the discharges reported here in more detail an $n = 1$, $m = 2$ mode is also evident from the Mirnov coil signals. The pellet penetrates to a minor radius of $r \approx 10-15$ cm, as measured with a D_β diagnostic (top view of the pellet path, 1D array).

0031-9007/94/72(26)/4093(4)$06.00

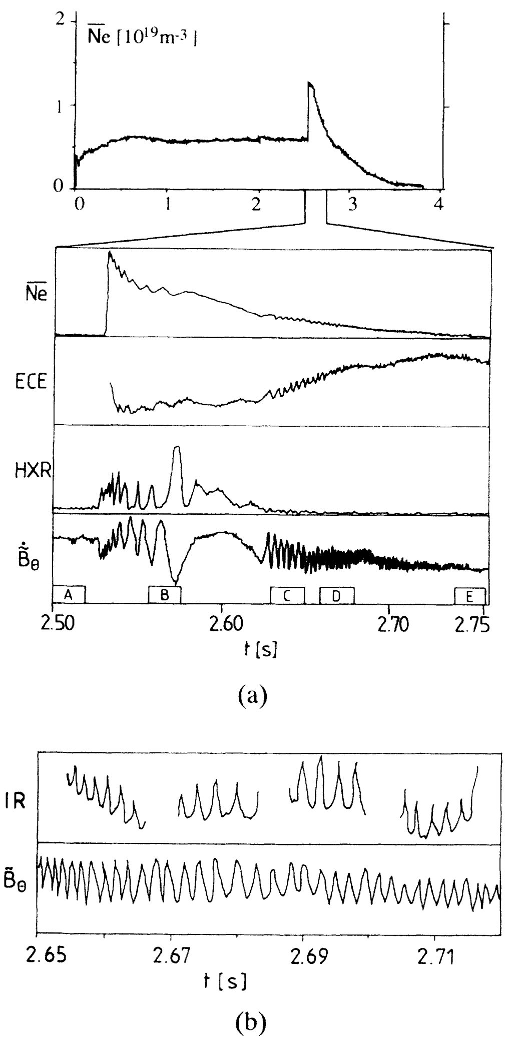

FIG. 1. (a) Density trace for a typical low density discharge containing a detectable amount of high energy runaways. At $t = 2.5$ cm a solid deuterium pellet is injected. This injection induces modulation of several signals. Shown are from top to bottom: line averaged electron density, ECE (thermal resonance at $r = -12$ cm), hard x-ray signal, and the Mirnov oscillations. The modulation sets in immediately after injection and decays within 200 ms. Indicated is also the times at which the pictures of Fig. 2 are recorded. (b) Oscillations on magnetics and on the synchrotron emission for a similar discharge as plotted in (a). The synchrotron emission is recorded in the line scan mode of the infrared camera, to obtain time information. Both signals have the same time structure.

As a result of the pellet injection the runaways undergo three distinct phases: (i) rapid loss, (ii) oscillation of the runaway radiation, and (iii) either a final loss or the formation of a stable runaway beam. These data will be analyzed first and the beam parameters will be derived. After that the transport aspects will be discussed.

(i) Rapid loss.—A large fraction of the runaway population is lost rapidly after injection. Using the IR camera in the line scan mode, it is observed that at the time of the pellet injection the synchrotron radiation in the central part decreases within about 0.6 ms. The runaways spread over the entire plasma cross section. After 0.6 ms most runaways have disappeared, and only a fraction of the runaways stay confined. In contrast to this rapid loss immediately following the pellet injection, for some discharges, such as the one presented in Fig. 1(a), the rapid runaway loss occurs about 50 ms after injection, as illustrated by the large burst of hard x rays. Note that this burst coincides with the locking of the magnetic modes. In four out of five discharges the remaining fraction is around 5%, whereas in one discharge it amounts to about 50%. In the latter case the density increase was significantly less than in the other cases. The remaining part is present in a plasma with high central density, of up to $5 \times 10^{19}\ \mathrm{m}^{-3}$.

(ii) Oscillation of synchrotron radiation.—After this initial loss, the synchrotron radiation observed in the normal camera mode (2D) exposes a spectacular picture. The spot of synchrotron radiation breaks up into many smaller, elongated ones (Fig. 2). This apparent filamentation of the synchrotron radiation goes on for several frames. While the size of these spots can vary in vertical extension, horizontally it is almost constant. For the interpretation it has to be considered that (i) the camera picture is built up in 1/60 s and contains therefore both space and time information and (ii) the synchrotron radiation is emitted into a narrow cone in forward direction. Therefore, if a bright spot repeatedly sweeps over the detector area within the 16.7 ms exposure time, the relatively slow line to line scanning results in the multiple spot picture. These considerations are confirmed by the 1D measurements. If one mirror is stopped the vertical direction contains only time information. The oscillations of the synchrotron radiation show the same time structure as the signals from the magnetic pickup coils, the interferometer, ECE, and several other diagnostics, see Fig. 1(b).

(iii) Stable beam.—The magnetic modes decay in about 0.2–0.3 s. At that time the synchrotron signal disappears completely in two cases, while in three other cases it forms one large spot again. This spot stays almost in the same position without change of intensity or extent over more than 0.6 s, i.e., up to the end of the discharge.

A helical $m = 1$ beam.—A number of physical parameters relevant for the runaway electrons still confined after pellet injection can directly be derived from the image. Because of the centrifugal force the relativistic electrons experience a vertical drift, meaning that their drift orbits are shifted to the low field side of the magnetic flux surfaces. This shift is given by

$$\delta = q p_{\|} / e B_{\phi} , \qquad (1)$$

whereby $q = r B_{\phi} / R B_{\theta}$ is the safety factor, $p_{\|}$ is the parallel momentum, e is the electron charge, and B_{ϕ} and B_{θ} are the toroidal and poloidal magnetic field components.

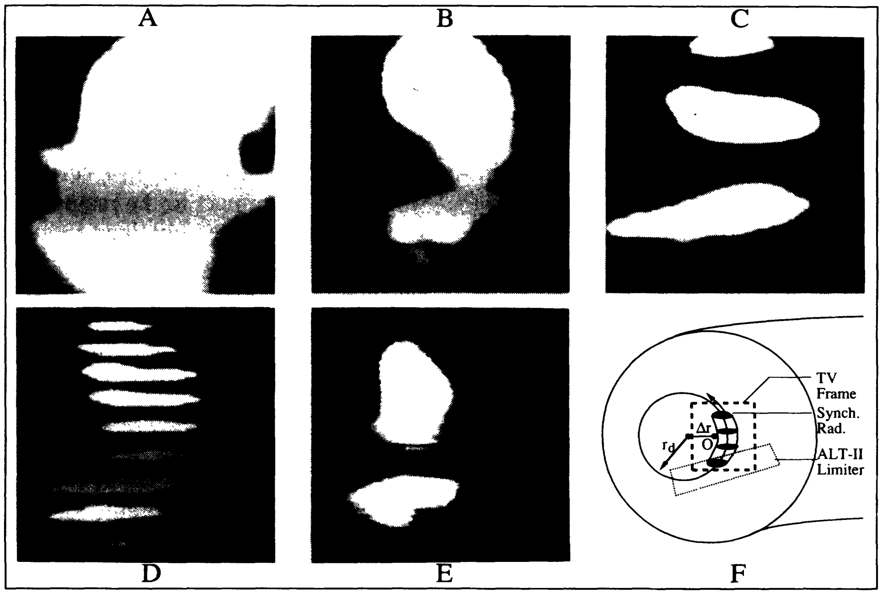

FIG. 2. Frames from the IR camera showing the synchrotron radiation at five different times, as indicated in Fig. 1. Frame A is recorded just before injection, B, C, and D show the oscillations of the synchrotron signal, coherent with the Mirnov oscillations. Frame E shows the situation when the magnetic modes have disappeared. F shows a sketch of the area observed with the IR camera.

Figure 2 shows that the spots of synchrotron light lie on a circle. The radius (r_d) and the center (Δr) of this circle, interpreted as a drift surface, are determined from the image: $r_d = 11 \pm 2$ cm, $\Delta r = 7.5 \pm 1.0$ cm. From soft x-ray measurements before pellet injection the inversion radius of the sawteeth was inferred to be $r_{\text{inv}} = 9 \pm 1$ cm. This leads to the conclusion that the synchrotron radiation originates from a beam of runaways at the $q = 1$ drift surface. The center of this surface is shifted to the low field side with respect to the geometrical center. Taking the Shafranov shift $s \approx 3.4$ cm into account, the displacement δ can be deduced: $\delta = \Delta r - s = 4 \pm 1$ cm. Using Eq. (1), this shift corresponds to an energy $E = 28 \pm 7$ MeV. This value agrees with the independent determination of E during the steady state before pellet injection [2].

The dimensions of the runaway beam can be determined from the image. The FWHM of the spot width (SW) is determined by the actual width of the beam (w) and the pitch angle θ (in the steady state before pellet injection determined to be $\theta = 0.12$): $\text{SW} = R\theta^2 + w$. Furthermore the poloidal length l_θ of the spot is determined as: $l_\theta \approx (2\pi r_d \Delta t_s/\Delta T) - R\theta^2$, where Δt_s is the time the spot is observed, and ΔT is the time between two successive spots. For one particular case we find: $w = 4{-}5$ cm, $l_\theta = 10 \pm 3$/cm. The volume of the runaway beam after injection is reduced to $(2.0 \pm 0.5)\%$ of the volume before injection ($r_{\text{beam}} \approx 25$ cm, see [3]). This value agrees with the intensity ratio of the synchrotron radiation before and after pellet injection, which was deduced to be $(4 \pm 2)\%$.

Transport results.—The radial and poloidal diffusion coefficients of the runaway electrons of 28 MeV in this helical beam can be determined from the behavior of these spots of synchrotron emission. The radial one is estimated from the small widening in time of the horizontal extent of the spots Δw: $D_r^{\text{re}} = (0.5\Delta w)^2/\Delta t \approx 1 \times 10^{-2}$ m^2/s. The poloidal diffusion coefficient is determined from the filling up of the gaps between the different spots, interpreted as the smearing out of the runaway beam over the drift surface. This yields $D_p^{\text{re}} = (0.5\Delta l_\theta)^2/\Delta t \approx 1.5 \times 10^{-2}$ m^2/s. We recall that after the magnetic perturbations have decayed, in some of the cases the runaways are still present, but smeared out poloidally over the flux surface. This thin shell is perfectly stable and stays at nearly the same position, without change of intensity, positions, or extent for more than 0.6 s. This stability is an indication of the very low diffusion rate of the runaway electrons.

The loss of runaways within 0.6 ms requires a diffusivity of $\chi_R \approx 300$ m^2/s during that period. In the same period, the loss of diamagnetic kinetic energy is only 5%, corresponding to a temporary increase of χ_{th} to only 20 m^2/s. This difference can be understood if the rapid loss of runaways is due to strong ergodization of the field. In this case, the diffusivity is an increasing function of the particle velocity. For a fully stochastic field, the ratio $\chi_R/\chi_{\text{th}} = v_R/v_{\text{th}}$ is predicted in [7]. This agrees well with the present observations, although it is not at all clear that the conditions for the validity of this theory are fulfilled. Note that the transport of runaways is compared to thermal transport: runaways are effectively test particles, not bound to the ion cloud by ambipolar fields.

As a possible explanation of the rapid loss of runaways a temporary strong ergodization of the magnetic field is considered. Because of the large orbit shift, the runaways are only sensitive to field fluctuations with large correlation length, i.e., low mode numbers. For the rapid loss it is further required that no good surfaces remain [8]. It is therefore hypothesized that the stochastization is due to overlap of large, low m magnetic islands. Such a situation would arise if the $m = 1$ and $m = 2$ islands grow very large, with possibly a $m/n = 3/2$ island squeezed in between. The width (w_2) and position (r_2) of the $m = 2$ island are estimated from the magnetic signals just before or just after the mode locks, yielding $w_2 \sim 8$ cm at $r_2 \sim 25$ cm. The width of the $m = 1$ island cannot be determined from the magnetic signals. However, the fact that the runaway beam survives the rapid loss phase, may be interpreted to show that this beam (width$\sim$shift$\sim$4 cm) is entirely enclosed inside the island. This yields an island width $w_1 \sim 12$ cm at $r(q = 1) = 9$ cm. Hence, already in the rotating phase, the islands cover $\sim 60\%$ of the separation between the resonant surfaces. Upon the short time of mode locking a further growth is expected, so that overlap may well occur. This is corroborated by the observation of a burst of HXR at the moment of mode locking. The fact that a runaway beam persists after the phase of rapid loss shows that in the chaotic sea there are still big remnant islands, at least of the $m = 1$ island. Thus, the overlap parameter may exceed unity, but the plasma is still far from the state of full stochasticity in which all remnants of islands are destroyed. Hence, even in the short period of high magnetic turbulence the plasma is still far from the fully stochastic regime which is prerequisite for a transport analysis such as due to Rechester and Rosenbluth [7].

Alternative explanations for the loss of snychrotron radiation that were considered were found inadequate. For example, slowing down through direct interaction with the pellet is estimated to give less than 1 MeV energy loss, which produces a negligible effect on the measurement. Pitch angle scattering would increase rather than decrease the synchrotron emission [3], and be obvious in the IR picture. Moreover, the observation that in some cases the loss does not occur simultaneously with the pellet penetration excludes these possibilities.

In conclusion, the observations of runaway electrons during and after pellet injection give rise to the following picture. After the passage of the pellet through the plasma a stochastic field forms. This is interpreted as caused by overlap of low m number magnetic islands. Runaway electrons are lost with an effective diffusivity of ≈ 300 m^2/s from this ergodic region. The bulk thermal diffusivity is much smaller, in agreement with predictions for transport in a fully stochastic field. Inside the big $m = 1$ island a beam of runaways survives the turbulent phase. This beam, a "drift island," is shifted by 4–5 cm with respect to the magnetic island. Whether the drift island must be contained in a larger magnetic island or that it can exist outside this, as expected from guiding center calculations [9, 10], is still an open question. The turbulent phase has a duration of only < 1 ms, during which the magnetic modes are locked. The short duration is essential to explain the modest loss of thermal energy. The persistent narrow runaway beam monitors the diffusion in the quiet phase after the rapid loss. In some cases it maintains an island topology, with radial and poloidal diffusivities that are extremely low, < 0.02 m^2/s. The radial diffusivity is equally small when the magnetic island decays and the runaways spread poloidally to form a thin shell.

Finally, there is a clear relation with the density "snake" observed in JET, a $m = n = 1$ helical tube of high density which occurs if a pellet penetrates to the $q = 1$ surface [11]. The density snake persists for hundreds of ms and even survives sawtooth crashes. Using this analogy, the phenomenon reported here could be called a "runaway snake."

This work was performed under the Euratom-FOM and Euratom KFA association agreement with financial support from NWO, KFA, and EURATOM.

[1] J. R. Myra *et al.*, Phys. Fluids B **4**, 2092 (1992).
[2] R. Jaspers *et al.*, Nucl. Fusion **33**, 1775 (1993).
[3] K. H. Finken *et al.*, Nucl. Fusion **30**, 859 (1990).
[4] K. H. Finken *et. al.*, Nucl. Fusion **32**, 915 (1992).
[5] R. Jayakumar, H. H. Fleischmann, and S. J. Zweben, Princeton Plasma Physics Laboratory Report No. PPPL 2849, 1992.
[6] K. N. Sato *et al.*, Proc. Int. Conf. Plasma Phys. **16C**, 403 (1992).
[7] A. B. Rechester and M. N. Rosenbluth, Phys. Rev. Lett **40**, 38 (1978).
[8] C. C. Hegna and J. D. Callen, Phys. Fluids B **5**, 1804 (1993).
[9] G. Fussmann *et al.*, in *Proceeding of the 7th International Conference Plasma Physics and Controlled Nuclear Fusion Research* (IAEA, Vienna, 1979), Vol. 1, p. 401.
[10] S. J. Zweben, B. V. Waddell, and D. W. Swain, Nucl. Fusion **20**, 477 (1980).
[11] A. Weller *et al.*, Phys. Rev. Lett. **59**, 2303 (1987).

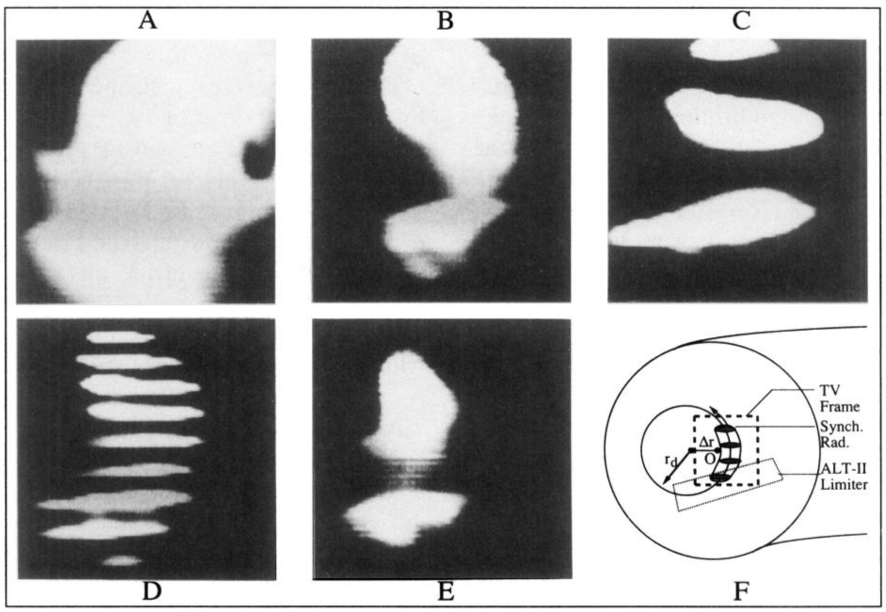

FIG. 2. Frames from the IR camera showing the synchrotron radiation at five different times, as indicated in Fig. 1. Frame A is recorded just before injection, B, C, and D show the oscillations of the synchrotron signal, coherent with the Mirnov oscillations. Frame E shows the situation when the magnetic modes have disappeared. F shows a sketch of the area observed with the IR camera.